

# Study of Leptonic and Semi-leptonic $B$ Decays at Belle

---

**Kevin Varvell**<sup>\*†</sup>

*The University of Sydney*

*E-mail:* [kevin.varvell@sydney.edu.au](mailto:kevin.varvell@sydney.edu.au)

Recent results from the Belle experiment on leptonic and semileptonic decays of  $B$  mesons are presented. The measurements are based on an integrated luminosity of  $711 \text{ fb}^{-1}$  collected at the  $\Upsilon(4S)$  resonance at the KEKB  $e^+e^-$  asymmetric collider.

*XIV International Conference on Heavy Quarks and Leptons (HQL2018)*

*May 27- June 1, 2018*

*Yamagata Terrsa, Yamagata, Japan*

---

<sup>\*</sup>Speaker.

<sup>†</sup>On behalf of the Belle Collaboration.

## 1. Introduction

Leptonic and semileptonic decays of  $B$  mesons provide an important tool for testing the predictions of the Standard Model of particle physics (SM), and in so doing searching for new physics beyond the SM. In particular the unitarity of the Cabibbo-Kobayashi-Maskawa (CKM) matrix, which governs charged weak coupling between quarks, can be explored. Each of the nine CKM matrix elements contributes to the coupling at a vertex linking a pair of quark flavours to the charged weak current ( $W^\pm$ ). In the context of  $B$ -meson decays, which allow the study of  $b \rightarrow W +$  lighter quark transitions, the binding of the  $B$  meson, and correlations with the final state particles, introduce complications due to strong interaction effects. These effects are somewhat simpler to handle theoretically for leptonic and semileptonic decays, which makes these decays attractive for study.

Five recent Belle studies of leptonic or semileptonic decays are presented here. All are based on a  $711 \text{ fb}^{-1}$  data sample that contains  $772 \times 10^6 B\bar{B}$  pairs, collected with the Belle detector at the KEKB asymmetric-energy  $e^+e^-$  (3.5 on 8 GeV) collider [1] operating at the  $\Upsilon(4S)$  resonance during the period 1999 - 2010. A detailed description of the Belle detector can be found in [2].

## 2. Experimental techniques

At Belle, reconstruction of  $B$ -meson decays exploits the relatively clean environment provided by the colliding electron and positron beams. The  $\Upsilon(4S)$  resonance to which the beam energies are tuned decays predominantly to  $B\bar{B}$  pairs. If one  $B$ -meson decays (semi)leptonically, and the other hadronically, the almost hermetic nature of the Belle detector allows, in principle, all final state particles to be reconstructed except the escaping neutrino(s). If only one neutrino is present, its 4-momentum can be directly estimated from the missing energy and momentum in the collision. In the case that a final-state  $\tau$  lepton producing at least one additional neutrino, it is still possible kinematically to achieve some separation of signal (semi)leptonic decays from backgrounds. Two

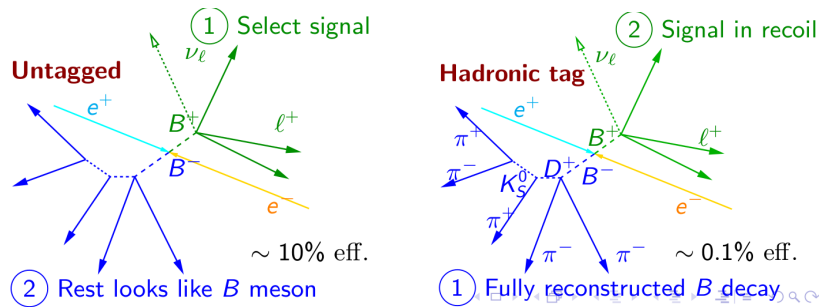


**Figure 1:** The two methods of reconstruction employed in the studies presented here - untagged (left) and full-reconstruction tagging (right), where in this example a purely leptonic  $B$  decay is the signal being sought. In the untagged case the signal  $B$  (minus neutrino) is reconstructed first, in the tagged case the tagging  $B$  is explicitly reconstructed first. The efficiencies given are indicative only and depend on the details of the particular analysis.

reconstruction scenarios are utilised in the studies presented here. In so-called “untagged” measurements, no attempt is made to reconstruct the  $B$  decay against which the signal  $B$  recoils in an

explicit, or exclusive decay mode. This method has relatively high efficiency but relatively low purity, as backgrounds are substantial and the resolution on the neutrino 4-momentum depends on the cumulative measurement uncertainties of the observed final-state particles in the collision. For “fully reconstructed (hadronic) tag” measurements, the non-signal  $B$  meson is reconstructed in one of over a thousand explicit decay channels, and the signal  $B$  meson searched for using the remaining particles in the event. In this case, very high purity and low backgrounds can be achieved, as well as tagging of the charge state of the  $B$ -meson pair. The trade-off is rather low efficiency, and possible tag bias if the properties of the tagging  $B$ -mesons are not well modeled by simulation. The two methods are illustrated in Figure 1 using the example of a purely leptonic signal  $B$  decay.

### 3. $B^+ \rightarrow \mu^+ \nu_\mu$ using an untagged technique

The purely leptonic decay is the simplest and cleanest of all  $B$  decays. Assuming a massless neutrino, in the SM the branching fraction (BF) is given by

$$\mathcal{B}(B^+ \rightarrow \ell^+ \nu_\ell) = \frac{G_F^2 m_B m_\ell^2}{8\pi} \left(1 - \frac{m_\ell^2}{m_B^2}\right)^2 f_B^2 |V_{ub}|^2 \tau_B$$

where  $G_F$  is the Fermi constant,  $m_B$  and  $m_\ell$  the masses of the  $B$ -meson and charged lepton ( $\ell = e, \mu, \tau$ ),  $V_{ub}$  is the relevant CKM matrix element,  $f_B$  is the  $B$  decay constant which can be calculated using Lattice QCD, and  $\tau_B$  is the lifetime of the  $B$  meson. The rarity of these decays makes them sensitive to physics beyond the SM. For example, in the case of  $B \rightarrow \tau \nu_\tau$ , a charged Higgs, as required by 2-Higgs doublet models, could contribute in place of the  $W$  boson in the decay, enhancing the BF. The decays to muon and electron have yet to be observed experimentally. Using reasonable inputs for the parameters  $|V_{ub}|$  and  $f_B$ , namely  $|V_{ub}| \times 10^3 = 3.74 \pm 0.14$  [3] and  $f_B = 0.186 \pm 0.004$  GeV [4], the SM prediction for the BF for the decay  $B \rightarrow \mu \nu$  is  $(3.80 \pm 0.31) \times 10^{-7}$ . The best current upper limit for this BF is  $10 \times 10^{-7}$  (HFLAV Dec 2017 average[5]).

The present analysis follows the untagged prescription. First a muon is selected, and then the rest of the event is checked for consistency with a  $B$ -meson decay on kinematic grounds. While the muon has a fixed momentum in the  $B$  rest frame, the boost to the  $\Upsilon(4S)$  frame results in a muon momentum  $p_\mu^*$  that varies from event to event. A neural network (NN) is used to separate signal from background, with the sidebands in  $p_\mu^*$  being used to validate the method. A signal efficiency of  $\sim 38\%$  is obtained. Once the signal region is unblinded, a fit in the 2-dimensional space of  $p_\mu^*$  versus the NN output variable  $o_{nn}$  is performed to extract the signal yield. The systematic uncertainties are reduced by, in fact, fitting to the ratio of the BF  $\mathcal{B}(B \rightarrow \mu \nu)$  to that for the semileptonic mode  $\mathcal{B}(B \rightarrow \pi \ell \nu)$ , which has been determined previously to reasonable precision.

The projections of the fit in the two variables  $o_{nn}$  and  $p_\mu^*$  in the signal-enhanced region are shown in Figure 2. The fitted yield for  $B \rightarrow \mu \nu$  is  $195 \pm 67$  events, which is consistent with the SM prediction while not being statistically significant enough to claim evidence for the decay. Expressed as a BF, the central value obtained is  $\mathcal{B}(B^+ \rightarrow \mu^+ \nu_\mu) = (6.46 \pm 2.22 \pm 1.60) \times 10^{-7}$  where the first uncertainty is statistical and the second systematic. This corresponds to a significance of  $2.4\sigma$ . Expressed alternatively as an interval, the result is  $\mathcal{B}(B^+ \rightarrow \mu^+ \nu_\mu) \in [2.9, 10.7] \times 10^{-7}$  at 90% C.L. This can be compared to the SM prediction of  $\mathcal{B}(B^+ \rightarrow \mu^+ \nu_\mu) = (3.80 \pm 0.31) \times 10^{-7}$ . Further details can be found in reference [3].

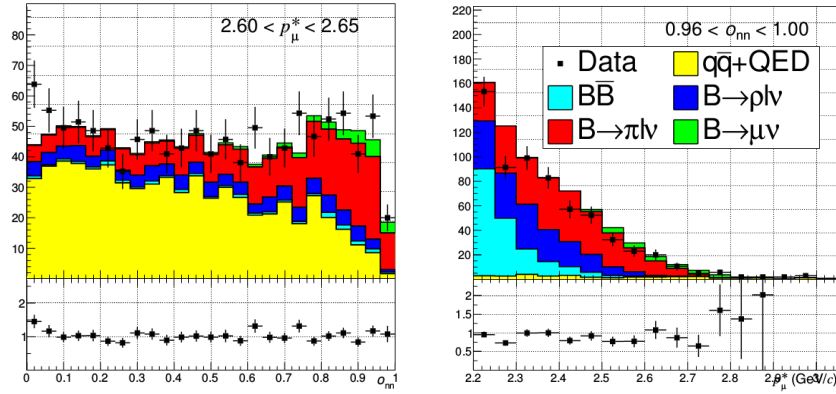


**Figure 2:** Projections of the fitted distribution of  $B \rightarrow \mu \nu$  onto the histogram axes in the signal-enhanced regions  $0.96 < o_{nm}$  and  $2.60 < p_{\mu}^* < 2.65$  GeV/ $c$ .

#### 4. $B^0 \rightarrow D^{*+} \ell^- \bar{\nu}_{\ell}$ using hadronic tagging

In this measurement, the hadronic tagging technique is employed to extract the total BF for the decay  $B^0 \rightarrow D^{*+} \ell^- \bar{\nu}_{\ell}$  ( $\ell = e, \mu$ ), along with a value for  $|V_{cb}|$ . A feature of the analysis is that unfolded differential BFs in four kinematical variables, namely, the recoil parameter  $w = (m_B^2 + m_{D^*}^2 - q^2)/(2m_B m_{D^*})$  and three helicity angles:  $\theta_{\ell}$ , the angle between the direction of the lepton and the direction opposite the  $B$  meson in the virtual  $W$  rest frame;  $\theta_{\nu}$ , the angle between the direction of the daughter  $D$  meson from the  $D^*$  and the direction opposite the  $B$  meson in the  $D^*$  rest frame; and  $\chi$ , the angle between the plane formed by the  $D^*$  decay and the plane formed by the  $W$  decay, defined in the  $B$  meson rest frame.

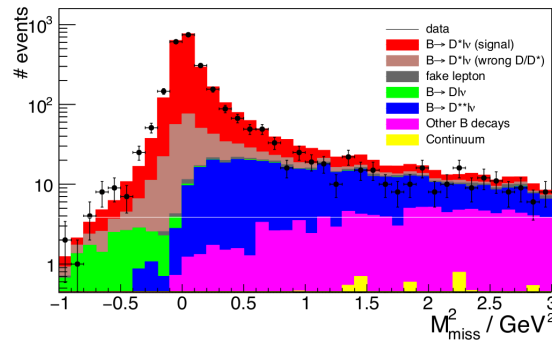


**Figure 3:** The  $M_{miss}^2$  distribution of all events after the  $B^0 \rightarrow D^{*+} \ell^- \bar{\nu}_{\ell}$  reconstruction.

After reconstructing a tagging  $B$  meson in a hadronic decay mode, a signal decay is searched for in the system recoiling against the tag. A lepton ( $e$  or  $\mu$ ) is selected, and  $D^0$  or  $D^+$  meson candidates are reconstructed in the decay modes  $D^0 \rightarrow K^- \pi^+$ ,  $D^0 \rightarrow K^- \pi^+ \pi^0$ ,  $D^0 \rightarrow K^- \pi^- \pi^+ \pi^+$ , or  $D^+ \rightarrow K^- \pi^+ \pi^+$ . These are then combined with a pion to reconstruct a  $D^{*+}$  meson candidate in the decay modes  $D^{*+} \rightarrow D^0 \pi^+$  or  $D^{*+} \rightarrow D^+ \pi^0$ . The missing mass squared  $M_{miss}^2$  is used to isolate

the signal. It is calculated from the missing 4-momentum in the event, constructed using the known beam 4-momenta and the 4-momenta of the tagging  $B$ ,  $D^*$  and lepton, and should peak at zero for signal since the missing 4-momentum would in this case be due to a single escaping neutrino.

The signal yield is obtained from an unbinned maximum likelihood fit to the  $M_{miss}^2$  distribution, from which the total BF for the decay can be estimated. The result is shown in Figure 3, with the fitted yield being  $2734 \pm 53$  events. The BF obtained is  $\mathcal{B}(\bar{B}^0 \rightarrow D^{*+} \ell^- \bar{\nu}_\ell) = (4.95 \pm 0.11 \pm 0.22) \times 10^{-2}$ , which can be compared with the world-average value from the HFLAV Summer 2016 compilation [6] of  $(4.88 \pm 0.01 \pm 0.10) \times 10^{-2}$ . Quoted uncertainties are statistical and systematic. Differential BFs and a value for  $|V_{cb}|$  are determined from a binned fit to the unfolded differential distributions of the four kinematical variables. The value of  $|V_{cb}|$  obtained is  $|V_{cb}| = (37.4 \pm 1.3) \times 10^{-3}$ , which can likewise be compared with the world average value [6] of  $(39.2 \pm 0.7) \times 10^{-3}$ . More details on this measurement can be found in reference [7]. This result complements the previous Belle untagged measurement [8].

### 5. $B \rightarrow D^{(*)} \pi \ell \nu$ using hadronic tagging

The decay mode  $B \rightarrow D^{(*)} \pi \ell \nu$  ( $\ell = e, \mu$ ) is an important background for measurements of the decay  $B \rightarrow D^{(*)} \tau \nu$ , and also helps in understanding the contributions to the inclusive BF for charmed semileptonic decays,  $\mathcal{B}(B \rightarrow X_c \ell \nu)$ . The process is expected to be dominated by the contribution of  $D^{**}$  decays. Following application of hadronic tagging, a muon or electron is selected from within the system recoiling against the tagging  $B$ , along with  $D^0$  and  $D^+$  candidates in 6 and 4 decay modes respectively. If the final state sought contains a  $D^*$ , candidates are reconstructed in the decay modes  $D^{*0} \rightarrow D^0 \pi^0$ ,  $D^{*+} \rightarrow D^+ \pi^0$  and  $D^{*+} \rightarrow D^0 \pi^+$ . Finally, a charged pion is combined with the lepton and  $D^{(*)}$  to form the complete final state excluding neutrino.

The signal is extracted by fitting to the the  $M_{miss}^2$  distribution, with the fitted distributions given in Figure 4. The obtained signal yields are  $515 \pm 31$  for  $B^+ \rightarrow D^- \pi^+ \ell^+ \nu$ ,  $571 \pm 40$  for  $D^{*-} \pi^+ \ell^+ \nu$ ,  $537 \pm 48$  for  $B^0 \rightarrow \bar{D}^0 \pi^- \ell^+ \nu$  and  $878 \pm 72$  for  $\bar{D}^{*0} \pi^- \ell^+ \nu$ . The BFs obtained are  $\mathcal{B}(B^+ \rightarrow D^- \pi^+ \ell^+ \nu) = (4.55 \pm 0.27 \pm 0.39) \times 10^{-3}$ ,  $\mathcal{B}(B^0 \rightarrow \bar{D}^0 \pi^- \ell^+ \nu) = (4.05 \pm 0.36 \pm 0.41) \times 10^{-3}$ ,  $\mathcal{B}(B^+ \rightarrow D^{*-} \pi^+ \ell^+ \nu) = (6.03 \pm 0.43 \pm 0.38) \times 10^{-3}$  and  $\mathcal{B}(B^0 \rightarrow \bar{D}^{*0} \pi^- \ell^+ \nu) = (6.46 \pm 0.53 \pm 0.52) \times 10^{-3}$  where the quoted uncertainties are statistical and systematic in each case. Further details can be found in reference [9].

### 6. $B \rightarrow \eta \ell \nu_\ell$ and $B \rightarrow \eta' \ell \nu_\ell$ using hadronic tagging

The charmless semileptonic BFs  $B \rightarrow \eta \ell \nu_\ell$  and  $B \rightarrow \eta' \ell \nu_\ell$  ( $\ell = e, \mu$ ) have been studied using hadronic tagging. Knowing the BFs for these decays helps in understanding the contributions to the inclusive BF for charmless semileptonic decays,  $\mathcal{B}(B \rightarrow X_u \ell \nu)$ .

Hadronic tagging is applied and the signal candidates are reconstructed requiring a lepton ( $e$  or  $\mu$ ), an  $\eta$  decaying either to  $\gamma\gamma$  or  $\pi^+ \pi^- \pi^0$ , or an  $\eta'$  decaying to  $\eta \pi^+ \pi^-$ . The signal is extracted by fitting to the  $M_{miss}^2$  distribution. The fitted distributions are given in Figure 4.

The measured BF for  $B^+ \rightarrow \eta \ell^+ \nu$  is  $\mathcal{B}(B^+ \rightarrow \eta \ell^+ \nu) = (4.2 \pm 1.1 \pm 0.3) \times 10^{-5}$ , obtained from a fitted yield of  $39 \pm 10$  events, with a significance of  $3.7\sigma$ . The quoted uncertainties are statistical and systematic. In the case of  $B^+ \rightarrow \eta' \ell^+ \nu$ , an upper limit is obtained of  $\mathcal{B}(B^+ \rightarrow$

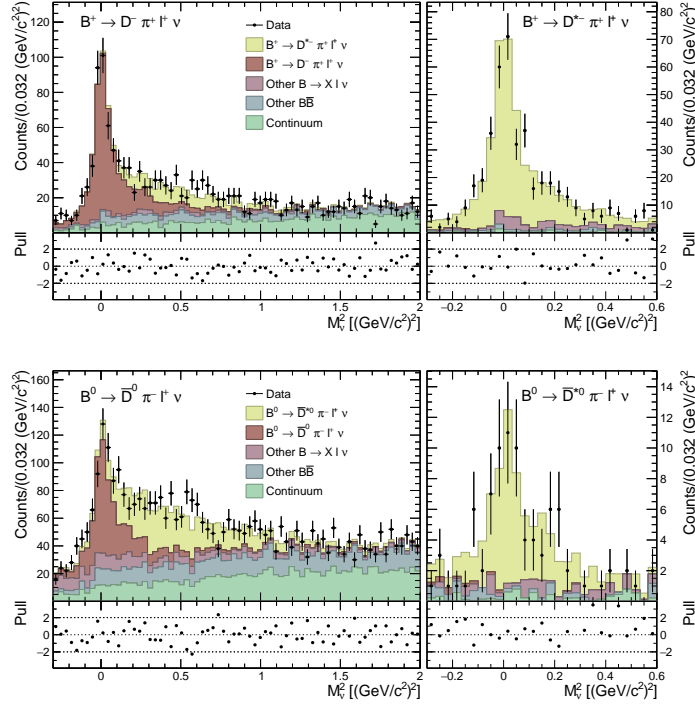


**Figure 4:** Binned extended maximum likelihood of the MC templates to the data for the combined fit to  $B^+ \rightarrow D^- \pi^+ \ell^+ \nu$  (top left),  $B^+ \rightarrow D^{*0} \pi^- \ell^+ \nu$  (top right),  $B^0 \rightarrow \bar{D}^0 \pi^- \ell^+ \nu$  (bottom left) and  $B^+ \rightarrow \bar{D}^{*0} \pi^- \ell^+ \nu$  (bottom right).

$\eta' \ell^+ \nu) < 0.72 \times 10^{-4}$  at 90 % C.L. As a check, a value for  $|V_{ub}|$  was extracted from the BF for  $B^+ \rightarrow \eta \ell^+ \nu$ , and found to be  $|V_{ub}| = (3.59 \pm 0.58 \pm 0.13^{+0.29}_{-0.32}) \times 10^{-3}$ , consistent with the value obtained from  $B \rightarrow \pi \ell \nu$  decays. The quoted uncertainties in this case are statistical, systematic and theoretical. Further details may be found in reference [10].

## 7. $R(D^*)$ in $\bar{B} \rightarrow D^* \tau^- \bar{\nu}_\tau$ and $\tau$ polarization using hadronic tagging

There is considerable interest at present in flavour anomalies such as those observed in semi-tauonic decays of  $B$  mesons, in particular through the measurement of

$$R(D^{(*)}) = \frac{\mathcal{B}(\bar{B} \rightarrow D^{(*)} \tau^- \bar{\nu}_\tau)}{\mathcal{B}(\bar{B} \rightarrow D^{(*)} \ell^- \bar{\nu}_\ell)}$$

where  $\ell = e, \mu$ . Measurements from the BaBar, Belle and LHCb experiments [12] are broadly consistent but deviate from SM expectations by several standard deviations. The polarisation of the  $\tau$  in  $\bar{B} \rightarrow D^{(*)} \tau^- \bar{\nu}_\tau$  decays is potentially sensitive to new physics. Belle has recently measured this polarisation for the first time, using hadronic tagging and, for the signal decays, the one-prong hadronic  $\tau$  decay modes  $\tau^- \rightarrow \pi^- \nu_\tau$  and  $\tau^- \rightarrow \rho^- \nu_\tau$ . Determining the helicity angle  $\theta_{hel}$ , defined as the angle between the visible products of the  $\tau$  decay in its rest frame and the direction of flight of the  $\tau$  in the  $W$  rest frame, is complicated by the fact that the  $\tau$  rest frame cannot be determined.

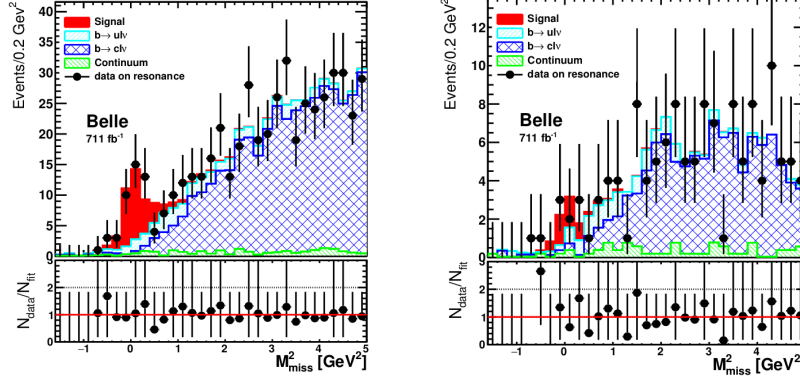


**Figure 5:** The fitted  $M_{miss}^2$  distribution for  $B \rightarrow \eta \ell \nu_\ell$  (left) and  $B \rightarrow \eta' \ell \nu_\ell$  (right).

The measurement exploits a kinematical relationship between the  $\tau$  and its daughters to gain access to this variable. Signal semitauonic events are separated from other processes utilising the residual energy in the electromagnetic calorimeter  $E_{ECL}$  not assigned to tag or signal  $B$  candidates, which should peak towards zero for signal events. The fitted distribution in this variable is shown in Figure 6 (left). The measured values for  $R(D^*)$  and  $P_\tau(D^*)$  are  $R(D^*) = 0.270 \pm 0.035^{+0.028}_{-0.025}$

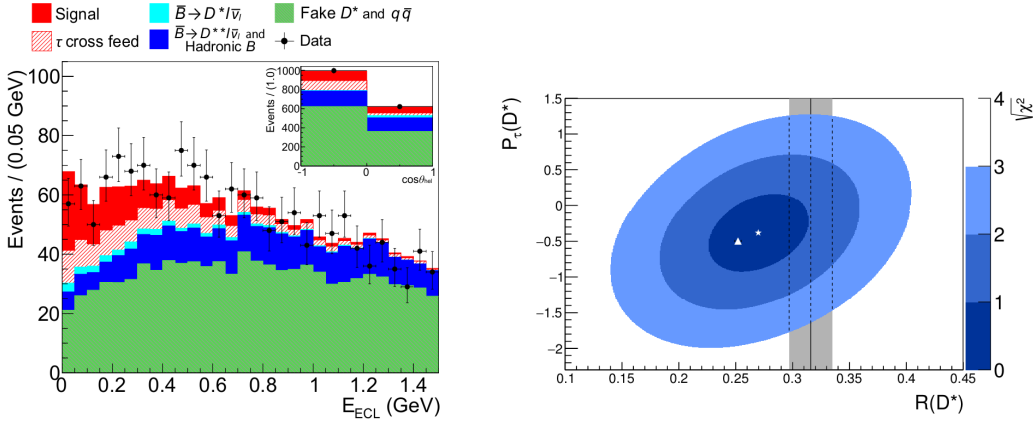


**Figure 6:** Left: Summed histogram of the  $E_{ECL}$  variable combining fit results to the eight signal samples (charged and neutral  $B$  decays, two  $\tau$  decay channels, and two  $\cos \theta_{hel}$  regions). The inset shows the summed histogram for the  $\cos \theta_{hel}$  variable combining the charged and neutral  $B$  decays and two  $\tau$  decay channels, for  $E_{ECL} < 1.5$  GeV. Right: Comparison of fit result (star for the best fit value and the contours for 1 to  $3\sigma$  regions) with the SM prediction (triangle). The grey region shows the average of the experimental measurements without the current result included [11].

and  $P_\tau(D^*) = -0.38 \pm 0.51^{+0.21}_{-0.16}$  where the uncertainties are statistical and systematic. These are consistent with SM predictions  $R(D^*) = 0.252 \pm 0.003$  [13] and  $P_\tau(D^*) = -0.497 \pm 0.013$  [14], as seen in Figure 6 (right). The full description of this analysis can be found in reference [15].



## 8. Conclusions

The full Belle dataset still continues to produce good physics. Recent results on five purely leptonic or semileptonic exclusive  $B$  decays have been described here. With the forthcoming Belle II experiment due to commence data-taking in 2019, prospects for much further progress in understanding of leptonic and semileptonic  $B$  decays can be anticipated in the future.

## References

- [1] S. Kurokawa and E. Kikutani, Nucl. Instrum. Methods Phys. Res. Sect., A **499**, 1 (2003), and other papers included in this Volume; T.Abe *et al.*, Prog. Theor. Exp. Phys. (2013) 03A001 and following articles up to 03A011.
- [2] A. Abashian *et al.* [Belle Collaboration], Nucl. Instrum. Methods Phys. Res. Sect. A **479**, 117 (2002).
- [3] A. Sibidanov *et al.* [Belle Collaboration], Phys. Rev. Lett. **121**, 031801 (2018). arXiv:1712.04123 [hep-ex].
- [4] S. Aoki *et al.* [FLAG Collaboration], Eur. Phys. J. C **77**, 112 (2017), arXiv:1607.00299 [hep-lat].
- [5] HFLAV December 2017 averages, <http://pdg.lbl.gov/2017/reviews/rpp2017-rev-hfag.pdf>.
- [6] Y. Amhis *et al.* [HFAG Collaboration], Eur. Phys. J. C **77**, 895 (2017), arXiv:1612.07233 [hep-ex].
- [7] A. Abdesselam *et al.* [Belle Collaboration], arXiv:1702.01521 [hep-ex].
- [8] W. Dungel *et al.* [Belle Collaboration], Phys. Rev. D **82**, 112007 (2010), arXiv:1010.5620 [hep-ex].
- [9] A. Vossen *et al.* [Belle Collaboration], Phys. Rev. D **98**, 012005 (2018), arXiv:1803.06444 [hep-ex].
- [10] C. Beleño *et al.* [Belle Collaboration], Phys. Rev. D **96**, 091102(R) (2017), arXiv:1703.10216 [hep-ex].
- [11] Y. Amhis *et al.* [HFAG Collaboration], arXiv:1412.7515 [hep-ex].
- [12] See for example HFLAV Summer 2018 averages, <https://hflav-eos.web.cern.ch/hflav-eos/semi/summer18/RDRDs.html>.
- [13] S. Fajfer, J. Kamenik, I. Nišandžić, Phys. Rev. D **85**, 094025 (2012), arXiv:1203.2654 [hep-ph].
- [14] M. Tanaka and R. Watanabe, Phys. Rev. D **87**, 034028 (2013), arXiv:1212.1878 [hep-ph].
- [15] S. Hirose *et al.* [Belle Collaboration], Phys. Rev. D **97**, 012004 (2018), arXiv:1709.00129 [hep-ex].